

## ELASTIC-PLASTIC SOLUTIONS FOR ANALYZING WELLBORE STABILITY

Mohamed Halafawi<sup>1</sup>

Lazăr Avram<sup>2</sup>

<sup>1</sup> PhD, Petroleum-Gas University of Ploiesti, **Romania**

<sup>2</sup> Professor and Dean of Oil & Gas Engineering Faculty, Petroleum-Gas University of Ploiesti, **Romania**

e-mail: halafawi\_2008@yahoo.com

DOI: 10.51865/JPGT.2022.01.04

### ABSTRACT

Selecting a good practical prediction method of wellbore instability has extensively become an important issue in order to overcome the resulting instability problems during drilling. Therefore, the aim of this paper is to simulate the actual stresses around wellbore using elastoplastic rock behavior in order to describe the actual cases of wellbore instability problems. The description of the stress state around wellbore, as well as common failure criteria are presented further in this paper. We also made a selection of the most applicable equations for description of stress state using elastoplastic rock behavior. Experimental data are used to calculate the cylindrical stresses surrounding the drilling hole wall at various diameters. Furthermore, a sensitivity analysis is done to test changing the radial stress with overbalance support and wellbore radius.

**Keywords:** Elastic-plastic rock, instability problems, stress state, radial stress, tangential stress.

### INTRODUCTION

In oil and gas fields, a stable borehole is drilled with different mud and completion brines so as to prevent the resulted well instabilities and casing damage problems that occur due to activities of drilling and production. These issues can occur due to a variety of circumstances and causes because of drilling activities and operations. For instance; the main causes may be various stress circumstances, well inclination and direction, deepwater processes, HPHT layers (high pressure, high temperature), anisotropic and non-homogenous pay zone, layer cuttings and drilling fluids interaction, and poor technologies and methods used [1,2]. To do a good analysis of borehole problems and issues like wall deterioration, mud losses, formation breaking-down, and fine sands migration towards wellbore; it is highly necessary to compute the Cartesian and cylindrical stresses circumstances surrounding drilling well walls [1,2].

Several authors have presented solutions and models for wellbore stability assuming linear elastic, non-linear elastic, poro-elastic, ideal plastic, plastic, or elastic-plastic rock behavior around the wellbore. However, few of them presented stress distribution and the description of wellbore behavior in elastic-plastic although it expresses the actual case that exists around the wellbore. This is because their equations are long and difficult to

be solved. Therefore, few of them solved these equations analytically and the most solved them numerically. Durban [3] presented a nonlinear problem of a spherical cavity surrounded by an infinite elasto-plastic medium, and subjected to uniform radial loads. Bratli [4] discussed elastic, plastic and elastic-plastic stress solutions, arch and wellbore model, for wellbore stability. Detournay [5] presented elastoplastic model of a deep tunnel for a rock with variable dilatancy. Durban [6] explained some related topics including a solid behaves as an elastic-perfectly plastic material, a thin-walled shell and the Mohr-Coulomb material. Peng [7] discussed wellbore stability while drilling and wellbore stability using elastic solution and elastoplastic solution. Fjaer [8] presented the borehole stability analysis for well design: Incorporating effects of nonlinear elasticity, plasticity and rock anisotropy. Integrating aspects of nonlinear elasticity theory, formation heterogeneity, and plasticity theory, Fjaer [8] analyzed the stability issues for wellbore construction. Pourhosseini [9] developed a constitutive model to describe the nonlinear behavior of intact rocks under static loading. This constitutive model contains the pre-peak elastic and the post-peak strain-softening behavior, as well as dilation.

A good understanding of the preceded various wellbore stability discussion, their techniques and calculations is essential for selecting good practical instability prediction method for overcoming the resulting drilling instability issues. Consequently, there is a growing need to create mathematical and numerical approaches, algorithms, and simulations to evaluate oil and gas wells difficulties caused by exploration activities. Petroleum production is tough due to harsh lithological conditions such as deepwater exploration and HPHT formations, the importance of a better and more precise stability comprehension of drilling wells grows exponentially. This is particularly true when drilling greatly inclined, underbalanced, and horizontal wells; and drilling into deeper and ambiguous or unexplored zones with a cracked rock naturally, as well as other geological difficulties.

Therefore, the aim of this paper is to simulate the actual stresses around wellbore using elastoplastic rock behavior in order to describe the actual cases, which previously explained, of wellbore instability problems. Description of stress state around wellbore is presented. Common failure criteria are also presented. Selection of the most applicable equations for description of stress state using elastoplastic rock behavior.

## **1. STATE OF STRESSES AROUND A WELLBORE**

Prior to any drilling of a borehole and assuming no adjacent seismic activities, the stress state of the rock layer is typically stable (static), with little or no tectonic activity. In this state, there are three major stresses known as in-situ stresses. The stationary stress conditions would be altered after drilling, resulting in hole instability issues. The drilled zone would subsequently be subjected to a variety of yields due to the unsymmetrical in-situ stress conditions. Figure 1 depicts the in-situ conditions of stresses that exist in the zone surrounding the wall of drilled hole. The first phase in making stability analysis of any rock zone is to identify this stress state. In order to study stress state around the wellbore, the insitu stress plate which represents the primary phase rock formation before drilling (Figure 1) must be converted to those shown in Figure 2-A [1].

The stress condition changes as a borehole is cut into the formation layer because the cylindrical wells produces a stress concentration that can reach a few inches away from

the wall. Because of the altered geometrical position, the stress state surrounding the borehole wall will be changed (Figure 2-B). In short, while boring into rock, there are two types of constraints to be considered: (1) in-situ stresses and (2) their distribution surrounding the well. The stress distribution surrounding the wellbore may surpass the rock strength, resulting in formation failures [1].

Identifying the pressures surrounding the wellbore during cutting formations, each rock type should also be identified. Additionally, the type of formation failure, which will happen, should be presented. Further, the suitable failure diagram of the rock formation should be described. Figure 3 shows the most common rock yield criteria during drilling activities and operations. Elevated formation pressure, a drilling disturbance induced into a stable zone, and probable chemical interactions between the drilling muds and rock are the major reasons of wellbore instability. Based on Figures 1 through 3, the stress state before and after drilling must be determined so as to do well design and stability analysis of the wellbore. Consequently, the general procedures of implementing a safely well design and stability study are illustrated in Flow Chart 4.

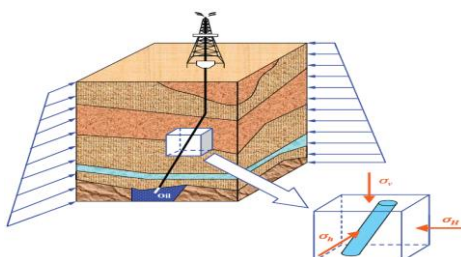


Figure 1. *In-situ stresses around a wellbore* [1].

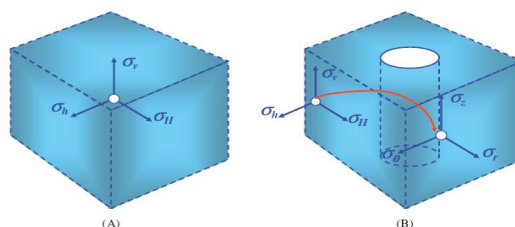


Figure 2: (A) *rock piece with a homogeneous stress state, and (B) rock layer with a distributed hole stress conditions* [1].

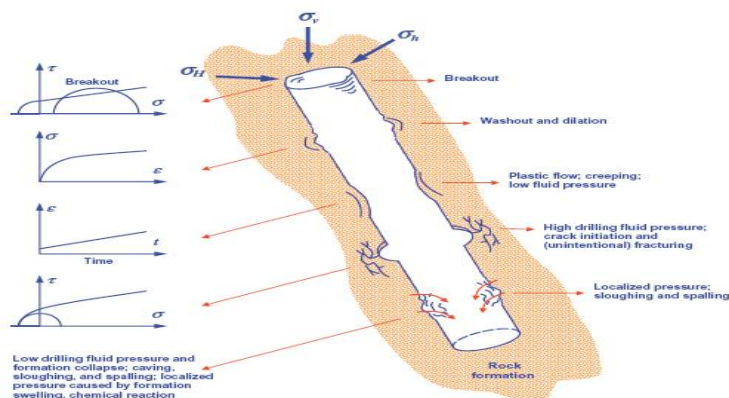


Figure 3. *Some instability problems during drilling* [2].

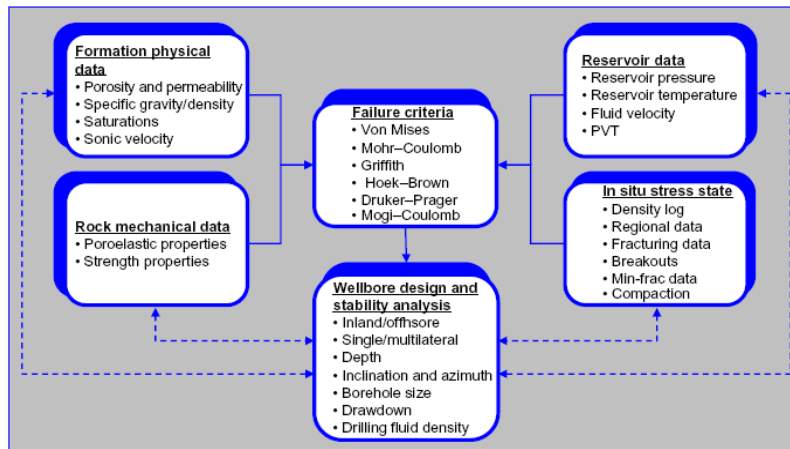


Figure 4. A general methodology for making hole design and stability analysis [1].

## 2. STUDY GENERAL ASSUMPTIONS

In the plotted cross section of the wellbore (Figure 5), the following assumptions are taken into consideration:

- Non-linear elastic, elastic-plastic stresses around the wellbore
- A non-linear elastic, and a plastic zone is formed surrounding the wellbore
- Different failure models used

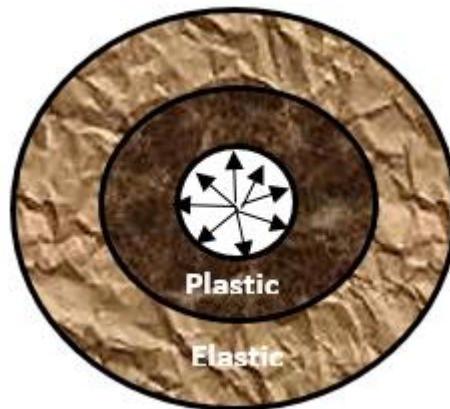


Figure 5. Wellbore schema.

## 3. ROCK FAILURE CRITERIA

In order to identify, clearly and definitely, stress conditions at rock failure, failure criteria are used. There are several failure criteria which are classified based on the middle stress and the behavior of rock (linear or no-linear). The common formation failure criteria are presented by authors [10,14] as shown in Table 1.

Table 1. Common rock failure criteria

Failure Criterion Name	Failure Criterion Formula
<b>Mohr-Coulomb</b>	$\tau = \mu\sigma + c, \mu = \tan\phi$ $\text{or } \sigma_1 = q\sigma_3 + C_o \quad \text{where } q = \frac{1+\sin\phi}{1-\sin\phi}, C_o = \frac{2c \cos\phi}{1-\sin\phi}$ <p>Where <math>c</math> is the rock cohesion, <math>\mu</math> is the coefficient of the internal friction angle (<math>\phi</math>), and <math>C_o</math> is the uniaxial compressive strength (UCS)</p>
<b>Mogi-Coulomb</b>	$\tau_{oct} = a + b \sigma_{m,2}$ $\tau_{oct} = \frac{1}{3} \sqrt{(\sigma_1 - \sigma_2)^2 + (\sigma_1 - \sigma_3)^2 + (\sigma_2 - \sigma_3)^2}, \sigma_{m,2} = \frac{1}{3} (\sigma_1 + \sigma_3)$ $a = \frac{2\sqrt{2}}{3} \frac{C_o}{q+1}, \quad b = \frac{2\sqrt{2}}{3} \frac{q-1}{q+1}$ <p>Where <math>\tau_{oct}</math> is octahedral shear stress and <math>\sigma_{m,2}</math> is mean normal stress</p>
<b>Tresca</b>	$\frac{(\sigma_1 + \sigma_3)}{2} = C = \tau_{max}, \quad \frac{C_o}{2} = C$ <p>Or as a special case of Mohr-Coulomb</p> $\sigma_1 = q\sigma_3 + C_o, \text{ when } \phi = 0,$ $q = \frac{1 + \sin\phi}{1 - \sin\phi} = 0 \text{ then } \sigma_1 - \sigma_3 = C_o$
<b>Von Mises</b>	$\sqrt{J_2} = \sqrt{\frac{(\sigma_1 - \sigma_2)^2 + (\sigma_1 - \sigma_3)^2 + (\sigma_2 - \sigma_3)^2}{6}} = \frac{C_o}{3}$ <p>Where <math>J_2</math> is the invariant of the deviatoric stress</p>
<b>Drucker-Prager</b>	$\sqrt{J_2} = k + \alpha J_1, \quad J_1 = \frac{\sigma_1 + \sigma_2 + \sigma_3}{3}$ $\alpha = \frac{3 \sin\phi}{\sqrt{9 + 3 \sin^2\phi}}, k = \frac{3 C_o \cos\phi}{2 \sqrt{q} \sqrt{9 + 3 \sin^2\phi}} \quad \text{for inscribed Drucker - Prager}$ $\alpha = \frac{\sqrt{3}(q-1)}{(2+q)}, k = \frac{\sqrt{3} C_o}{(2+q)} \quad \text{for Circumscribed Drucker - Prager}$ <p>Where <math>k</math> and <math>\alpha</math> are the material constants and related to the cohesion of rock and frictional angle of rock, and is the mean effective <math>J_1</math> confining stress</p>
<b>Hoek-Brown</b>	$\sigma_1 = \sigma_3 + \sqrt{m C_o \sigma_3 + s C_o^2}$ <p>Where <math>m</math> and <math>s</math> are constant depending on both rock and fracture properties and parameter <math>s</math> for intact rock is equal to 1</p>
<b>Lade &amp; Modified Lade</b>	$\left(\frac{I_1^3}{I_3} - 27\right) \left(\frac{I_1}{p_a}\right)^m = \eta_1 \quad \text{where } I_1 = (\sigma_1 + \sigma_2 + \sigma_3), I_3 = (\sigma_1 \sigma_2 \sigma_3) \quad \text{for Lade}$ <p>Where <math>m</math> and <math>\eta_1</math> are material constants, <math>p_a</math> is atmospheric pressure and <math>I_1, I_2</math> are the stress invariant parameters</p> $\frac{I_1^3}{I_3} = \eta_1 + 27 \quad \text{for Modified Lade}$ <p>where</p> $I''_1 = (\sigma_1 + S) + (\sigma_2 + S) + (\sigma_3 + S)$ $I''_3 = (\sigma_1 + S) \cdot (\sigma_2 + S) \cdot (\sigma_3 + S)$ $S = \frac{c}{\tan\phi}, \eta = \frac{4 \tan^2\phi (9 - 7 \sin\phi)}{(1 - \sin\phi)}$
<b>Modified Wiebols-Cook</b>	$\sqrt{J_2} = A + B J_1 + C J_1^2$ $C = \frac{\sqrt{27}}{2C_1 + (q-1)\sigma_3 - C_o} \left( \frac{C_1 + (q-1)\sigma_3 - C_o}{2C_1 + (q-1)\sigma_3 - C_o} - \frac{q-1}{q+2} \right)$ $C_1 = (1 + 0.6\mu)C_o$ $B = \frac{\sqrt{3}(q-1)}{q+2} - \frac{C}{3} [2C_o + (q-1)\sigma_3]$ $A = \frac{C_o}{\sqrt{3}} - \frac{C_o}{3} B - \frac{C_o^2}{9} C$

<b>Griffith</b>	$\text{In } (\tau - \sigma) \text{ plane, } \tau^2 = 4T_0(\sigma + T_0)$ $(\sigma_1 - \sigma_3)^2 = 8T_0(\sigma_1 + \sigma_3)$ $\sigma_3 = -T_0 \quad \text{IF } (\sigma_1 + 3\sigma_3) < 0, \text{ and } T_0 = \frac{C_0}{8}$
<b>Modified Griffith</b>	$\sigma_1 \left[ \frac{\sqrt{\mu^2 + 1} - \mu}{4} \right] - \sigma_3 \left[ \frac{\sqrt{\mu^2 + 1} + \mu}{4} \right] = 4T_0$ $4T_0 = \frac{C_0}{\sqrt{\mu^2 + 1} - \mu}$
<b>Murrel</b>	$(\sigma_1 - \sigma_3)^2 + (\sigma_1 - \sigma_2)^2 + (\sigma_2 - \sigma_3)^2 = 24T_0(\sigma_1 + \sigma_2 + \sigma_3)$ <p><i>In terms of octahedral stresses, <math>\tau_{oct}^2 = 8T_0 \sigma_{oct}</math></i></p> $T_0 = \frac{C_0}{12}$ <p>Where <math>\sigma_{oct}</math> is equal to mean confining stress <math>J_1</math></p>
<b>Stassi d'Alia</b>	$(\sigma_1 - \sigma_3)^2 + (\sigma_1 - \sigma_2)^2 + (\sigma_2 - \sigma_3)^2 = 2(C_0 - T_0)(\sigma_1 + \sigma_2 + \sigma_3) + 2C_0T_0$

#### 4. ELASTIC-PLASTIC STRESSES

When a borehole is drilled to an intact formation, a plastic zone is formed in the vicinity of the borehole, covering a few borehole diameters before an in-situ elastic zone appears, as shown in Figure 2. During drilling activities, the plastic region may generate many well instability issues. Because of hydrocarbon production, the plastic region in the study area may spread deeper into an oil or gas reservoir, resulting in producing sand. Borehole wall yield may occur in fractured rocks unless a heavy mud weight is applied. For applications like borehole, operations of perforation, and sand extraction, the extent of the plastic region must be evaluated [11]. Bray [12] established the premise which microfractures with shaped log spirals at deviated angles  $\delta$  in the radial direction form in the plastic range (Figure 6). Furthermore, Goodman [11] provided an overview of stresses surrounding the hole wall for elastic-plastic formation behavior, and they are briefly expressed as following:

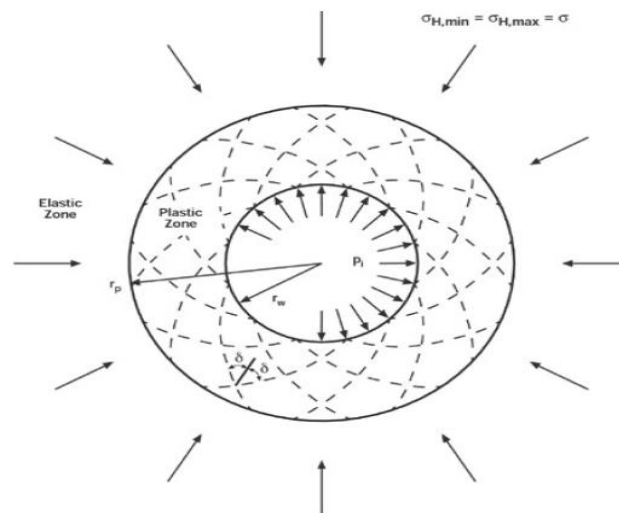


Figure 6. The description of plastic and elastic areas based Bray's assumption [11].

We will analyze a theoretical model given by Bray [11] to acquire a stronger insight to provide a mathematical model for determining efficient wall upholding techniques by studying the physics of a borehole wall. According to the Mohr-Coulomb theory, the

well's construction generates undesirable stress issues, leading the rock to yield. The simple assumption that the condition of stress is axisymmetric, that is,  $K=1$ , is made to allow the study of the extent of breakdown, the plastic region. Bray presumed inside this zone that the micro-fractures would be log spirals shaped at circular  $\delta$  degrees in the direction of wellbore radii, which extends to radius  $r_{pl}$ , as anticipated by a rigorous application of the Mohr-Coulomb theory (Figure 6). This method is ineffective for many rocks, because the fissures will create spiral cracks parallel to the hole walls and floor. However, Bray's hypothesis is considered an applicable suggestion for clay and shaly formations. The appropriate value of  $\delta$  for minimal strength is  $45 + \phi / 2$ , but the value of  $\delta$  will be treated as a solution's self-supporting parameter. It could be used to specify a quantity  $Q$  as follows:

$$Q = \frac{\tan \delta}{\tan(\delta - \phi_j)} - 1 \quad (1)$$

The radius of  $r_{pl}$  of the elastic-plastic zone is provided by Equation 2 supposing that the yield formation inside the plastic region has shear strength spiral patterns,  $\tau_p = S_j + \sigma \tan \phi_j$ .

$$r_{pl} = r_w \left[ \frac{2 \sigma' - C_o + \left[1 + \tan^2 \left(45 + \frac{\phi}{2}\right)\right] S_j \cot \phi_j}{\left[1 + \tan^2 \left(45 + \frac{\phi}{2}\right)\right] (P_i + S_j \cot \phi_j)} \right]^{1/Q} \quad (2)$$

Where  $\sigma'$  is the original rock stress ( $\sigma_v = \sigma_h = \sigma'$ ),  $C_o$  is the rock unconfined compressive strength,  $p_i$  is the wellbore internal pressure provided by the supports, and  $\phi$  is the rock internal friction angle. If we apply the Mohr-Coulomb and assuming  $\sigma_{Hmin} = \sigma_{Hmax} = \sigma'$ , and in terms of the experimentally determined cohesion for jointed rocks ( $C_j$ ), pressure difference between drilling fluid and pore pressure ( $P_w - P_r$ ), and the internal friction angle for jointed rocks ( $\phi_j$ ); the radius of the plastic zone,  $r_{pl}$ , will be:

$$r_{pl} = r_w \left[ \frac{2 \sigma' - C_o + \left(1 + \frac{1 + \sin \phi}{1 - \sin \phi}\right) C_j \cot \phi_j}{\left(1 + \frac{1 + \sin \phi}{1 - \sin \phi}\right) (P_w - P_r) + C_j \cot \phi_j} \right]^{1/Q} \quad (3)$$

and

$$\sigma'_v = g \int_0^H \rho_b dH - \alpha P_r \quad (4)$$

Although field measurements is the best technique to calculate stress, if laboratory is un-obtainable, we can use the following approximation:

$$\sigma'_v = 1.1 H - \alpha P_r \quad (5)$$

The effective  $\sigma_{Hmin}$  and  $\sigma_{Hmax}$  can also be estimated as follows, assuming an elastic, tectonic activity relaxed, and transverse confined formation:

$$\sigma'_{H,min} = \frac{\nu}{1-\nu} \sigma'_v \quad (6)$$

$$\sigma'_{H,max} = \frac{\sigma'_v + \sigma'_{H,min}}{2} \quad (7)$$

Where  $P_b$  is the formation overburden bulk density and  $H$  is the depth. Bray's solution for cylindrical stresses inside the elastic and plastic zones is provided by:



$$\sigma'_r = \sigma' - r_{pl} \left[ \frac{\left( \frac{1+\sin\phi}{1-\sin\phi} - 1 \right) \sigma' + C_o}{r^2 \left( \frac{1+\sin\phi}{1-\sin\phi} + 1 \right)} \right] \quad (8)$$

$$\sigma'_{\theta\theta} = \sigma' - r_{pl} \left[ \frac{\left( \frac{1+\sin\phi}{1-\sin\phi} - 1 \right) \sigma' + C_o}{r^2 \left( \frac{1+\sin\phi}{1-\sin\phi} + 1 \right)} \right] \quad (9)$$

For the elastic zone, and

$$\sigma'_{rr} = ((P_w - P_r) + C_j \cot \phi_j) \left( \frac{r}{r_w} \right)^Q - C_j \cot \phi_j \quad (10)$$

$$\sigma'_{\theta\theta} = ((P_w - P_r) + C_j \cot \phi_j) \frac{\tan \delta}{\tan(\delta - \phi_j)} \left( \frac{r}{r_w} \right)^Q - C_j \cot \phi_j \quad (11)$$

For plastic zone

The radially inward displacement,  $u_r$  is given by:

$$u_r = \frac{1-\nu}{E} \left( P_i \frac{r_w^{Q+1}}{r^Q} - P_r \right) + \frac{t}{r_w} \quad (12)$$

Where

$$t = \frac{1-\nu}{E} r_{pl}^2 \left[ (\sigma' + S_j \cot \phi_j) - (p_i + S_j \cot \phi_j) \left( \frac{r_{pl}}{r} \right)^Q \right] + \frac{1-\nu}{E} b \quad (13)$$

$$b = \left( \frac{[1 + \tan^2(45 + \frac{\phi}{2})] \sigma' + C_o}{\tan^2(45 + \frac{\phi}{2}) + 1} \right) \quad (14)$$

## 5. EXPERIMENTAL DATA

A rock sample is taken from a wellbore wall where a plastic area formed surrounding a borehole wall with micro-cracks, with internal friction angle of joint = 30° and no joint cohesion, and log spirals inclined with 45° of joint. Table 2 lists the mechanical characteristics of the elementary rock. The in-situ stresses are also given Table 2.

Table 2. *Experimental data of rock sample* [11]

Parameter	Value	Unit
Cohesion of joint, $C_j$	0	
Internal friction angle of joint, $\phi_j$	30	degrees
Log spirals inclined of joint, $\delta$	45	degrees
Mechanical properties of the virgin rock mass		
Compressive strength, $C_o$	1300	Psi
Internal friction angle, $\phi$	39.9	degrees
$\sigma_{Hmin} - \sigma_{Hmax}$	4000	Psi
$P_w - P_r$	40	Psi
Young Modulus, $E$	$10^7$	Psi
Possion's ratio	0.2	-
Rock density	150	Lb/ft <sup>3</sup>

If the plastic region must be solidified in a weakly consolidated structure, these statistics are critical. The zone can be investigated as a skin caused by the formation's plastic deformation via well-testing. The stresses displacements in the elastic and plastic regions will be determined based on Bray's solution. A sensitivity analysis will be done to study the effect of fluid support and wellbore radius on rock displacement.

## 6. RESULTS AND ANALYSIS

Wellbore stability are studied and simulated by using elastoplastic equations presented by Goodman [11]. Also, the Bray solution proposed for these equations was used. Additionally, the experimental data (Table 2) presented by Goodman [11] was utilized surrounding the wellbore to describe cylindrical stresses (i.e tangential & radial stresses). The cylindrical stresses surrounding the borehole wall are depicted in Figures 7 through 10 in case of elastoplastic rock behavior for different radii around the borehole wall (Figures 5 & 6). Figure 11 shows also the comparison of these stresses with various borehole diameters. Obviously, the trendlines firstly appear in Figures 7 through 11 is completely different from which presented by Kirsch equations [1,11-13]. These equations for elastic rock behavior and result in decreasing tangential stress and increasing radial stress around wellbore to a certain point. Then, both of them starts to be constant with a wider distance from the wellbore. However, there is a small area formed around the wellbore and behaves as plastic materials, and then it behaves as elastic materials. This happens due to the effect of formation pressure and the drilling fluid density.

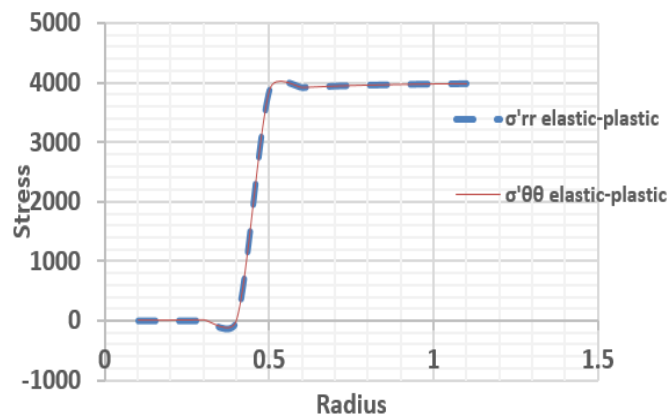


Figure 7. Cylindrical stresses (tangential and radial) for elastic-plastic case ( $r_w=1$ ).

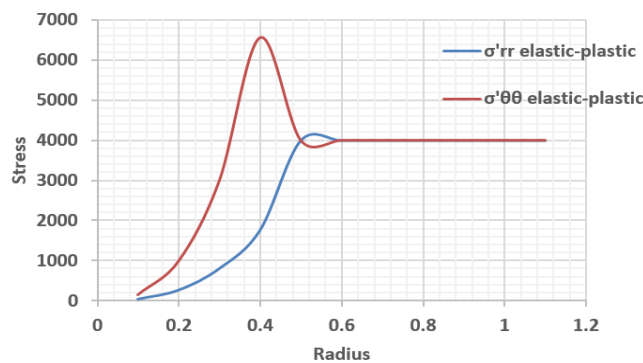


Figure 8. Cylindrical stresses (tangential and radial) for elastic-plastic case ( $r_w=0.1$ ).

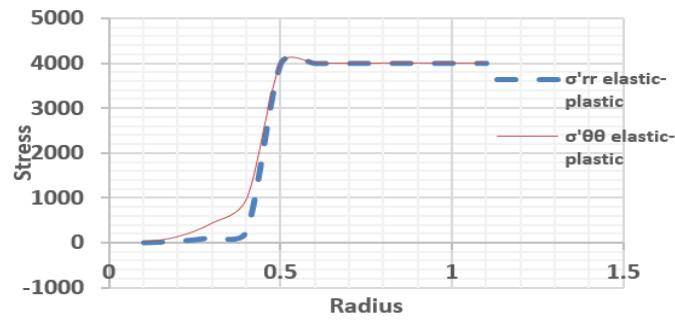


Figure 9. Cylindrical stresses (tangential and radial) for elastic-plastic case ( $r_w=0.2$ ).

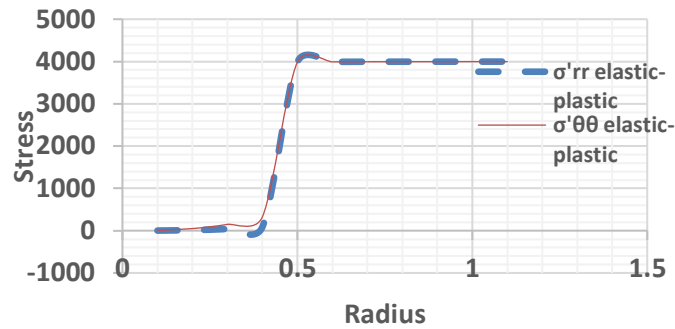


Figure 10. Cylindrical stresses for elastic-plastic case ( $r_w=0.3$ ).

### Stress vs. $r/r_w$

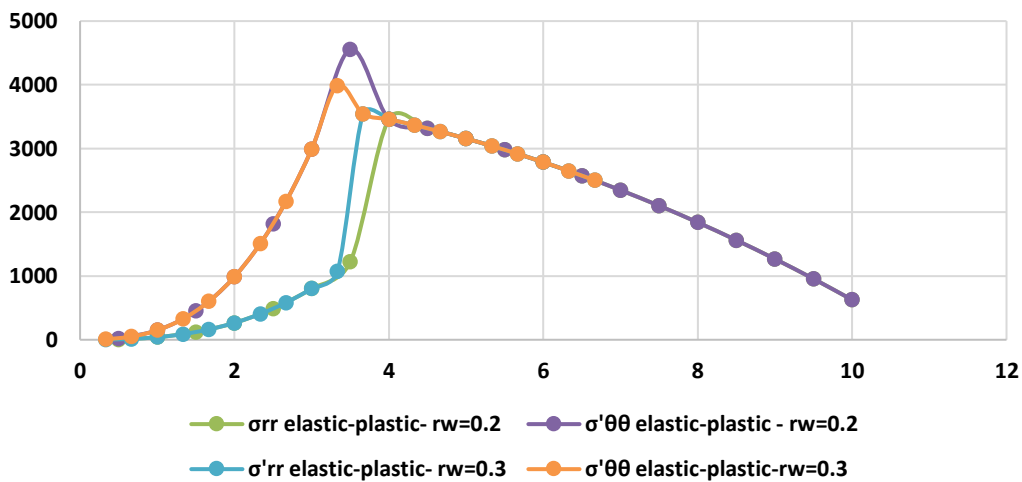


Figure 11. Comparison of wellbore stresses for various hole diameters.

Further, changing the diameter of wellbore means that various hole section to be drilled. It is clear that both stresses are significantly important and may lead to borehole wall failure or yield. However, the most important is the tangential stress which may reach to a higher values than radial stress as shown in Figures 7 through 11. Hence, this requires a higher mud density to stabilize the wellbore during drilling (Figures 8 & 11). Moreover, drilling geological sections with higher diameter results lower tangential stresses that those of lower diameters and they require therefore lower mud densities which is logically correct (Figure 11). Therefore, drilling lower sections of higher depths needs higher

densities of drilling fluids. Regarding the rock displacement, the radial displacement decreases with increasing the the drilling fluid support pressure (Figure 12). The more radial displacement, the higher wellbore/radius surrounding the rock plastic zone (Figure 13). Thus, the elasto-plastic rock behavior represents the actual wellbore wall behavior during drilling and helps to select the best mud weight and trajectory for safely passing all rock zones.

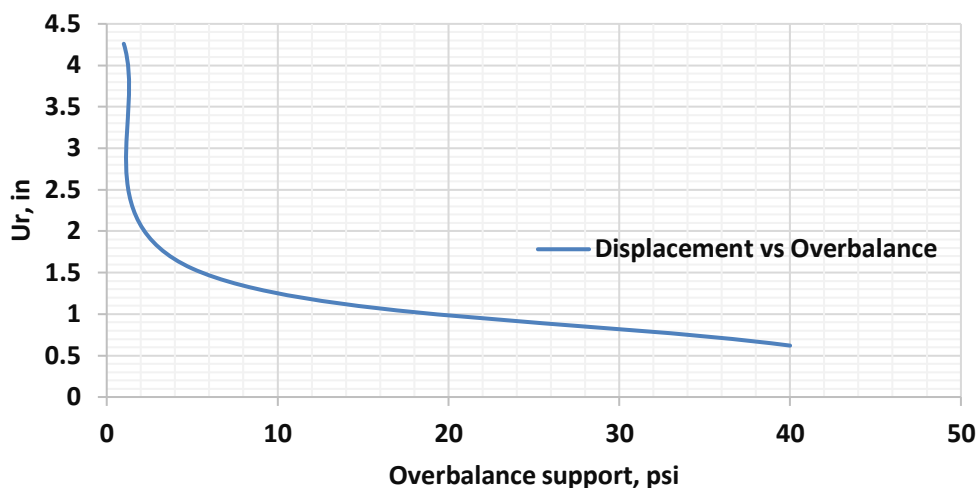


Figure 12. Changing of radial displacement with overbalance support.

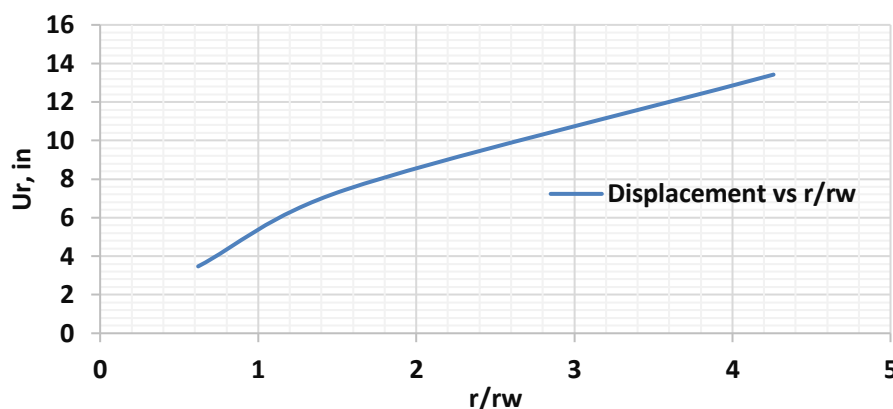


Figure 13. Variation of radial displacement with r/rw.

## CONCLUSIONS

Based on the results and analysis, the following conclusions and recommendations are extracted:

1. Elastoplastic rock behaviour represents the actual situation occurred during drilling geological layers.
2. Calculated stresses from elastoplastic case consider the optimum stresses for selecting the appropriate drilling fluid properties.
3. The larger hole diameter is, the lower tangential and radial stresses are, and the lower mud densities require.



4. Although this study is done based on experimental data, it can be done if the logging data are available.
5. Although elastoplastic calculations are quite complex, they give the most accurate and optimum results.

## REFERENCES

1. Aadnøy B.S., Loyeh R., Petroleum rock mechanics: drilling operations and well design, 2nd Edition, Gulf Professional Publishing, Elsevier Inc., 2019
2. Economides M.J., Watters, L.T., Dunn-Norman, S., Petroleum well construction, John Wiley, 1998.
3. Durban, D., Baruch, M., On the Problem of a Spherical Cavity in an Infinite Elasto-Plastic Medium. *J. Appl. Mech.* Dec 1976, 43(4): 633-638. 1976.
4. Bratli, R.K., Horsrud, P., Risnes, R., Rock mechanics applied to the region near a wellbore. 5th ISRM Congress, Melbourne, Australia, pp. 1-17. 1983.
5. Santareli, F.J. and Brown, E.T., Performance of deep boreholes in rock with a confining pressure dependent elastic modulus, *Proc. 60 Int. Society of Rock Mech.* Vol. 2: 1217-1222. Balkema, Rotterdam. 1987.
6. Durban, D., Fleck, N.A, Spherical Cavity Expansion in a Drucker-Prager Solid. *J. Appl. Mech.* Dec 1997, 64(4): 743-750. 1997.
7. Peng S., Zhang J., *Engineering Geology for Underground Rocks*, Springer-Verlag Berlin Heidelberg, 2007
8. Fjaer, E., Holt, R., Raaen, A.M., Horsrud, P., and Risnes, R., *Petroleum Related Rock Mechanics*, second edition. *Developments in Petroleum Science*, 53. Amsterdam: Elsevier Science Publishers. 2008
9. Pourhosseini O., Shabanimashcool M., Development of an elasto-plastic constitutive model for intact rocks, *International Journal of Rock Mechanics & Mining Sciences*, 66, 1–12, 2014.
10. Halafawi, M., Avram, L., Borehole Insitu Stress Stability Analysis of RBS-9 Field Utilizing the Inversion Technique. *Journal of Engineering Sciences and Innovation, Petroleum and Mining Engineering Section (F)*, Vol. 4, Issue 1. 2019.
11. Goodman, R.E., *Introduction to Rock Mechanics*, John Wiley & Sons, 1980.
12. Bray, J.A., *Study of Jointed and Fractured Rock – Part II, Felsmechanik and Ingenieur geologic*, Volume 4, 1967.
13. Guangquan Xu, *Wellbore Stability in Geomechanics*, PhD thesis, University of Nottingham, 2007.
14. Rahimi, R., Nygaard, R., What Difference Does Selection of Failure Criteria Make in Wellbore Stability Analysis?, *ARMA 14-7146, 48th US Rock Mechanics / Geomechanics Symposium held in Minneapolis, MN, USA, 1-4 June 2014.*